Molecular Packing of Polyesters Derived from 1,4-Butanediol and Even Aliphatic Dicarboxylic Acids

Ahmed Almontassir, Sebastià Gestí, Lourdes Franco, and Jordi Puiggalí*

Departament d'Enginyeria Química, Universitat Politècnica de Catalunya, Av. Diagonal 647, E-08028, Barcelona, Spain

Received January 9, 2004; Revised Manuscript Received May 4, 2004

ABSTRACT: The crystalline structures of polyesters 4 8, 4 10, and 4 12 have been studied using X-ray and electron diffraction and real space electron microscopy. They belong to the series of polyesters derived from 1,4-butanediol and even-dicarboxylic acids. This work allows the previously reported data on polyesters 4 4 and 4 6 to be extended. The new polymers adopt an all-trans conformation and pack according to orthorhombic unit cells that contain four molecular segments. This feature contrasts with the smaller unit cells reported for other poly(alkylene dicarboxylate)s which have also an all-trans conformation. Molecular simulation has been used to calculate the diffraction patterns and determine the main packing features. Lamellar crystals with a truncated lozenge morphology are obtained by isothermal crystallization of dilute alcohol solutions. A regular folding habit on the different lamellar sectors is evident by using polyethylene decoration techniques. Thin films of negative birefringent spherulites are obtained by melt crystallization and their electron diffraction patterns studied.

Introduction

Extensive studies concerning the structure of aliphatic polyamides have been carried out[1] since their synthesis was reported by Carothers.[2] Different structures have been reported and related to the chemical repeat units,[3] i.e., the methylene ratio and the kind of polyamide (odd, even, odd−odd, even−even, odd−even). However, other families of condensation polymers, such as polyesters, have not been studied so extensively. Recent applications of these polymers as biodegradable materials[4] have enhanced the interest in the structure of these polyesters. Poly(ester amide)s have recently become another group of polymers with a potential use as biomaterials due to the combination of degradability and properties.[5−7] The knowledge of the structure of the parent polymers, both polyamides and polyesters, is useful for the understanding of the structure of the poly(ester amide)s.[8]

Aliphatic polyesters may be classified into two main groups depending on the kind of repeating units: poly(hydroxy alkanoate)s and poly(alkylene dicarboxylate)s. The structure of some polyesters in the first group has been widely studied owing to their major reported applications as both commodity (i.e., poly-ϵ-caprolactone[9]) and speciality (i.e., polyglycolide,[10] polylactide[11−13] and poly(*R*)-3-hydroxybutyrate[14]). Direct diffraction methods have even been used to analyze the electron diffraction data from poly-ϵ-caprolactone,[15] suggesting a molecular packing similar to that of polyethylene but with a slight distortion from a planar zigzag conformation. Polymers with lateral groups show more twisted conformations and, in some cases, polymorphism[11−13] and also frustrated crystalline structures.[16]

Poly(alkylene dicarboxylate)s are usually referred as polyesters *n m* since they obey to the chemical formula $-[O(CH_2)_nOCO(CH_2)_{m-2}CO]-$. Kink conformations based on a pair of gauche bonds with opposite signs placed on the diol or the dicarboxylic units have been proposed for some ethylene glycol, succinic, and adipic derivatives.[17−19] However, an almost all-trans conformation appears to be the most stable when molecules are constituted by long polymethylene sequences.[20] Molecular packing has been reported for only a limited number of poly(alkylene dicarboxylate)s. In general monoclinic or orthorhombic unit cells have been found,[1] the parameters of the *c*-chain axis projected unit cells ($a \approx 0.51$ nm, $b \approx 0.73$ nm) being close to those reported for the orthorhombic structure of polyethylene. Space groups have been determined in a few cases, in general being assumed that the two molecular segments of the unit cell are related by an *a*-glide plane perpendicular to the *b*-axis.[19] Nevertheless, recent studies carried out with polyesters 6 10[21] and 12 10[22] have demonstrated the existence of an *n* diagonal glide plane. This kind of symmetry has some implications for the folding geometry in different sectors in regular chain-folded lamellar crystals.

Of the poly(alkylene dicarboxylate)s, poly(tetramethylene succinate) (BIONOLLE) is currently receiving considerable attention owing to its commercial interest as a degradable material. Polymorphism has been observed, and $T_7GT\bar{G}$ (α form[23]) and T_{10} (*β* form[24]) conformations have been reported. Furthermore, crystal structure analyses indicate a monoclinic $P2_1/n$ space group for both structures.[25] Poly(tetramethylene adipate) is another butanediol derivative that shows polymorphism, as suggested by Minke and Blackwell.[26,27] In this case, an all-trans conformation (*β* form) has also been reported, but the diffraction data also showed a disorder along the chain axis that made it impossible to determine the space group symmetry. The second structure (α-form) shows a nonextended conformation for the diol units.[28]

The main purpose of this work is to progress into the structural studies of polyesters derived from 1,4-butanediol and even-dicarboxylic acids. Thus, suberic (PE 4 8), sebacic (PE 4 10), and dodecadioic (PE 4 12) derivatives are studied, since structural data are not available for this series with long polymethylene segments.

* To whom correspondence should be addressed. E-mail: jordi.puiggali@upc.es.

10.1021/ma049939l CCC: $27.50
Published on Web 06/16/2004

Experimental Section

Polyesters 4 8, 4 10, and 4 12 were synthesized from the appropriate dicarboxylic acid using an excess of 1,4-butanediol (molar ratio 2.2/1) by thermal polycondensation in a vacuum at 180 °C with titanium tetrabutoxide as a catalyst. Yields were in the 75−85% range. Intrinsic viscosities were measured with a Cannon-Ubbelhode microviscometer in dichloroacetic acid solutions at 25 ± 0.1 °C. Values of 0.85, 1.20, and 0.60 dL/g were determined for polyesters 4 8, 4 10, and 4 12, respectively.

Basic calorimetric data were obtained using a Perkin-Elmer DSC-PYRIS 1 differential scanning calorimeter; indium metal was used for calibration. Heating runs were performed at 20 °C/min. The melting temperatures were 61, 63, and 72 °C for polyesters 4 8, 4 10, and 4 12, respectively. The fusion temperature of PE 4 10 is in agreement with previously reported data (60,[29] 62,[30] and 67 °C[31]).

Isothermal crystallizations were carried out in the 30−55 °C range from dilute solutions (0.01% w/v) in alcohols such as *n*-butanol and *n*-hexanol. The crystals were recovered from mother liquor by centrifugation, repeatedly washed with *n*-butanol, and deposited on carbon-coated grids that were shadowed with Pt−carbon at an angle of 15° for bright field observations. Alternatively, when very thin crystals were obtained, a drop of the solution was placed on the grid, and the solvent was allowed to evaporate to avoid crystal breakage during centrifugation. Polymer decoration was achieved by evaporating polyethylene onto the surface of single crystals, as described by Wittmann and Lotz.[32]

Spherulites were prepared by crystallization from the melt. A small film fragment was placed between a coverslip and a slide and heated above the melting temperature using a Linkam THMS 600 hot stage. The upper glass was pressed to squeeze the melt into a thin film and then cooled rapidly to the desired crystallization temperature. A Carl Zeiss Standard GFL optical microscope and a first-order red tint plate were used to determine the sign of spherulite birefringence in cross-polarization conditions. After mechanical separation of the two glasses, the spherulites attached to the coverslip were covered with a thin carbon film, floated off on water, and picked up on copper grips for electron microscopy observations. Optical micrographs were taken with an Olympus Camedia C-3040.

Oriented samples suitable for electron diffraction were also prepared on benzoic acid or on poly(tetrafluoroethylene) substrates by epitaxial crystallization by following the technique previously used for polyesters.[33,34] Highly birefringent zones of these films were selected under the polarizing microscope and transferred onto EM grids.

A Philips TECNAI 10 electron microscope was used and operated at 80 and 100 kV for bright field and electron diffraction modes, respectively. Selected area electron diffraction patterns were recorded on Kodak Tri-X films. The patterns were internally calibrated with gold ($d_{111} = 0.235$ nm). Electron diffraction patterns were digitized, and the intensity of reflections was determined by means of the ELD program.[35] This also allowed the intensity of saturated reflections to be estimated by a shape fitting procedure. A curve-fitting algorithm is used by the program to estimate what the reflection intensity would be if the spot were saturated by assuming the tail to be a Gaussian type function.

X-ray patterns were recorded under vacuum at room temperature, using calcite as a calibration standard. A modified Statton camera (W. R. Warhus, Wilmington, DE) with Ni−Cu radiation of wavelength 0.1542 nm was used. Fibers or films were prepared from the melt and annealed under stress at 50 °C. X-ray diffraction patterns were digitized and the intensity of reflections determined by means of the ICE software package provided by CCP13.[36] Intensities were corrected for area, Lorentz, and polarization factors. Patterns were also recorded from mats of single crystals, prepared by slow filtration of a crystal suspension on a glass filter. The X-ray beam was directed perpendicular to the stretching direction for films and fibers, whereas it was parallel to the mat surface in the study of sedimented crystals.

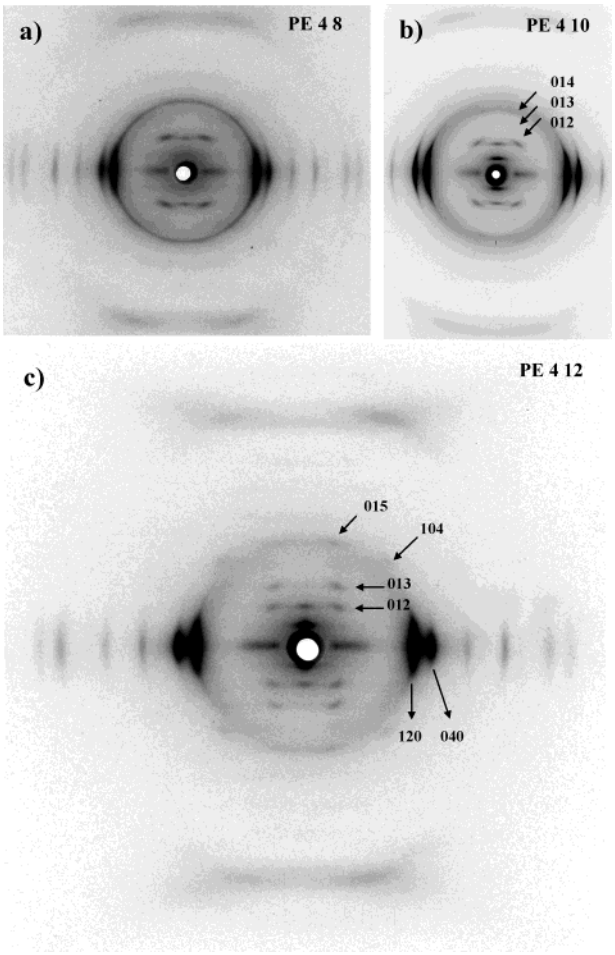

Figure 1. X-ray fiber diffraction patterns of polyester 4 8 (a), 4 10 (b), and 4 12 (c) showing the labeling of the main reflections.

The density of fibers was measured at 25 °C by the flotation method in mixtures of ethanol and CCl_4. Values of 1.15, 1.10, and 1.06 dL/g were determined for polyesters 4 8, 4 10, and 4 12, respectively.

Structural modeling was carried out by means of the diffraction software package of the Cerius^2 (Accelrys Inc.)[37] computer program. Charge distribution was calculated by the charge equilibration panel of Cerius^2 using a small representative molecule. All these calculations were run on a Silicon Graphics Indigo Workstation.

Results and Discussion

X-ray Diffraction Results. Figure 1 shows the fiber diffraction patterns of the three polyesters studied, whereas the main observed reflections are summarized in Table 1. The three patterns are similar, and the reflections index on orthorhombic unit cells with dimensions $a = 0.506$ nm, $b = 1.462$ nm, and c (chain axis) = 1.72 nm, $a = 0.505$ nm, $b = 1.460$ nm, and c (chain axis) = 1.97 nm, and $a = 0.506$ nm, $b = 1.456$ nm, and c (chain axis) = 2.22 nm for the derivatives of suberic, sebacic, and dodecanodioic acid, respectively. The chain axis repeats correspond to a fully all-trans conformation; an increase in the *c*-value close to 0.25 nm (two methylene groups) is found along the series.

A 2/*m* molecular symmetry characterizes the even−even polyesters with an all-trans conformation (Figure 2a). Inversion centers are placed in the middle of both diol and dicarboxylic units. In addition, binary axes perpendicular to the molecular chain axis pass through

Table 1. Measured and Calculated X-ray Diffraction Spacings (nm) for Polyesters 4 *n*

	polyester 4 8		polyester 4 10		polyester 4 12	
index[a]	measd[b]	calcd	measd[b]	calcd	measd[b]	calcd
120	0.416 vs E	0.416	0.415 vs E	0.416	0.415 vs E	0.415
040	0.365 vs E	0.365	0.365 vs E	0.365	0.364 vs E	0.364
140	0.296 m E	0.296	0.296 m E	0.296	0.296 m E	0.295
200	0.250 s E	0.253	0.251 s E	0.252	0.255 s E	0.253
220	0.239 vw E	0.239	0.239 vw E	0.239	0.239 vw E	0.239
160	0.219 w E	0.220	0.218 w E	0.219	0.220 w E	0.219
240	0.208 w E	0.208	0.206 w E	0.207	0.209 w E	0.208
001	1.71 w M	1.71	1.97 vs M	1.97	2.22 vs M	2.22
002	0.858 m M	0.860	0.986 s M	0.985	1.11 m M	1.11
012	0.737 s off M	0.741	0.815 s off M	0.816	0.882 m off M	0.883
003					0.738 vw M	0.740
013	0.534 vw off M	0.533	0.597 vw off M	0.599	0.659 m off M	0.660
014	0.414 vw off M	0.413	0.468 vw off M	0.467	0.517 w off M	0.519
015	0.335 vw off M	0.335	0.378 vw off M	0.380	0.422 m off M	0.425
104					0.377 vw off M	0.374
025	0.315 vw off M	0.311				
026					0.330 vw off M	0.330
027	0.230 m M	0.233			0.290 vw off M	0.291
107	0.222 s off M	0.221				
028			0.231 m M	0.233	0.259 w off M	0.259
108			0.221 s off M	0.221		
029					0.233 m M	0.234
039					0.219 s off M	0.220

[a] On the basis of orthorhombic unit cells with $a = 0.506$ nm, $b = 1.462$ nm, and $c = 1.72$ nm, $a = 0.504$ nm, $b = 1.460$ nm, and $c = 1.97$ nm, and $a = 0.506$ nm, $b = 1.456$ nm, and $c = 2.22$ nm for polyesters 4 8, 4 10, and 4 12, respectively. [b] Abbreviations denote relative intensities and orientations: vs, very strong; s, strong; m, medium; w, weak; vw, very weak; M, meridional; E, equatorial; off M, off meridional.

the inversion centers and a mirror plane contains all carbon atoms.

The space group symmetry of poly(alkylene dicarboxylate)s with almost fully all-trans conformations and long polymethylene segments has been reported in some cases.[19] In this way, a $P2_1/n11$ space group and a unit cell containing two molecular segments (Figure 2b) have been determined for the poly(dodecamethylene sebacate).[22] The structure can be described using the axial shift and the value of the setting angle, τ, of a molecular chain (i.e., number 1 in Figure 2b), which is usually close to 45°.

A common feature of the polyesters studied in this work is the relatively high value of the *b* parameter. This implies that the unit cell contains four molecular segments. In this way, densities of 1.19, 1.17, and 1.15 g/mL can thus be calculated for polyesters 4 8, 4 10, and 4 12, respectively, being in reasonable agreement with the measured values. Different 01*l* reflections are clearly visible in the X-ray fiber diffraction patterns, specifically for the most oriented sample of polyester 4 12. These spots constitute the clearest evidence of a molecular packing defined by a larger unit cell. To our knowledge, this is the first time that this kind of packing has been reported for aliphatic polyesters with all-trans conformations.

All *hk*0 equatorial reflections can be indexed (Table 1) with even *k* values, which implies the existence of a *b* glide plane perpendicular to the *c*-chain axis direction. In this way, the *c*-chain axis projection could also be defined by a conventional rectangular unit cell with the *b* parameter close to 0.73 nm. A $P2_1ab$ space group appears to be the only one possible if an orthorhombic symmetry, a setting angle different from 0 or 90°, an all-trans conformation, and the presence of 01*l* reflections are considered. A representation of the molecular packing with labeling of symmetry elements is shown in Figure 2c. Note that molecules 1 and 3 (as well as

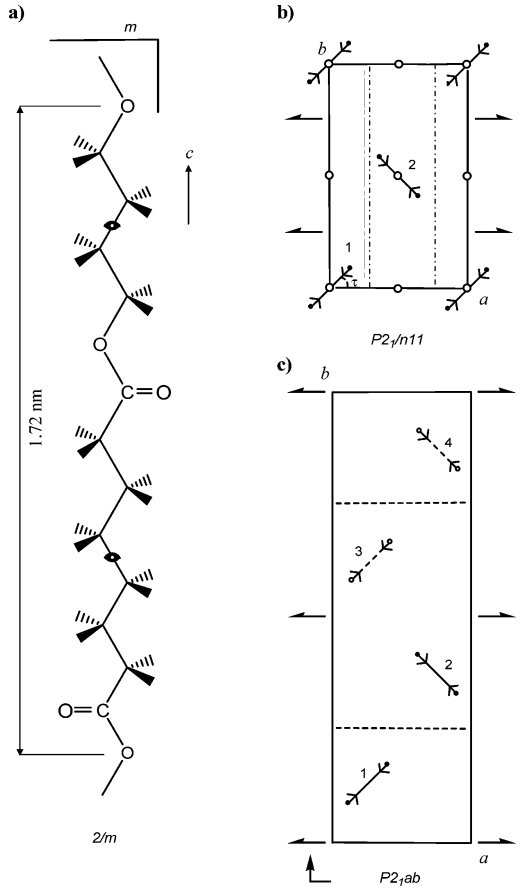

Figure 2. (a) Schematic representation showing the symmetry of a polyester 4 8 molecular chain with an all-trans conformation. (b) Projection along the *c*-axis of the molecular packing of a polyester with a $P2_1/n$ symmetry. (c) Projection along the *c*-axis of the molecular packing of a polyester with a $P2_1ab$ symmetry. In this case molecules related by the *b*-glide plane are differentiated by the solid and dashed line representations.

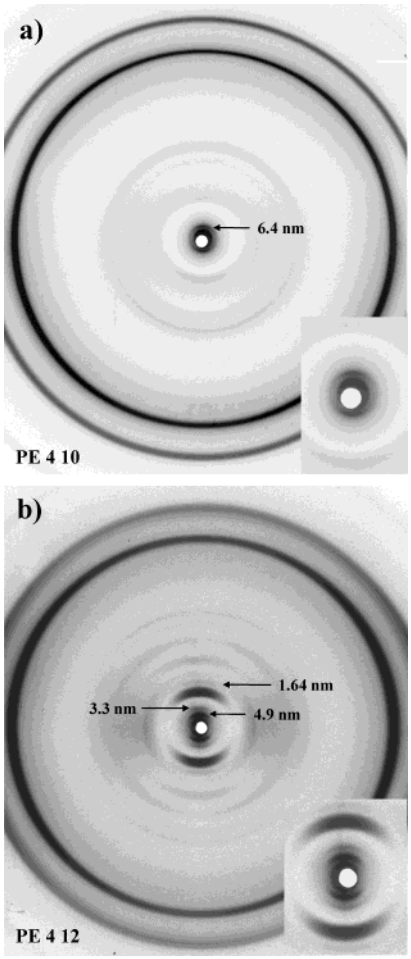

Figure 3. X-ray diffraction patterns of sedimented crystal mats of polyester 4 10 (a) and 4 12 (b) obtained by isothermal crystallization in *n*-hexanol at 40 and 55 °C, respectively. Insets show the first lamellar periodicity observed at 6.4 nm for polyester 4 10 and the second, third, and sixth orders of 9.9 nm for the lamellar periodicity for polyester 4 12.

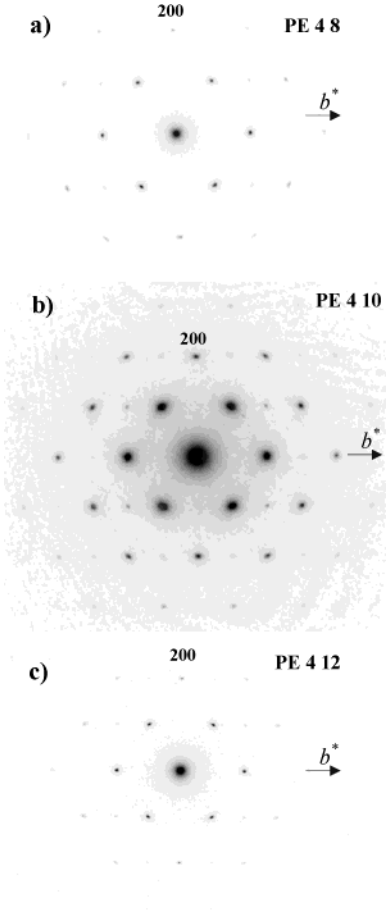

Figure 4. Electron diffraction patterns of single crystals of polyester 4 8 (a), 4 10 (b), and 4 12 (c).

molecules 2 and 4) are identical in the *c*-chain axis projection, giving rise to a reduced unit cell.

Inspection of fiber patterns shows the presence of some *h*0*l* reflections with *h* odd (i.e., 104 in Figure 1c), which is not in accordance with the systematic absence rule of the indicated space group. Thus, symmetry needs to be changed to a monoclinic space group (*P*11*b*) that allows the degrees of freedom of the structure to be increased.

X-ray diffraction patterns of sedimented crystal mats (Figure 3) confirm that solution grown crystals have the same structure as that observed for fibers. Only new low-angle reflections associated to lamellar thickness can be observed. This thickness appears sensitive to the crystallization conditions as will be explained below.

Electron Diffraction Results. Figure 4 shows the *hk*0 electron diffraction patterns obtained from the solution grown lamellar single crystals. These must be chain-folded taking into account that molecular chains are oriented perpendicular to the crystal basal plane, the lamellar thickness is reduced, and the samples have high molecular weights.

The electron diffraction patterns are characterized by a 2*mm* symmetry and define rectangular unit cells (Table 2), whose *a* and *b* parameters are in agreement with those deduced from the fiber X-ray diffraction patterns. Some features are worth highlighting:

(a) *h*00 and 0*k*0 systematic absences with *h* odd and *k* odd are detected when a small unit cell with *b* equal to 0.73 nm is considered. In this case, a rectangular *p*2*gg* planar group derives and the azimuthal setting angles of molecules 1 and 2 (Figure 2c) are related by the symmetry elements. This observation confirms that molecules tend to pack according to the $P2_1ab$ space group. However, minimization of the packing energy causes a chain axis shift between molecules 1 and 2 that reduces the symmetry to the indicated *P*11*b* space group.

(b) No systematic absences with $h + k$ odd can be detected. Thus, the projected unit cell is not centered and the azimuthal setting angle must be different from 0 or 90°.

To enhance the electron diffraction data obtained from solution grown single crystals, epitaxial crystallizations were performed. However, similar *hk*0 electron diffraction patterns were attained again when benzoic acid (Figure 5a) or poly(tetrafluoroethylene) (Figure 5b) was used as a substrate.

Morphological Features of Solution-Grown Lamellar Crystals. Isothermal crystallization in dilute alcohol solutions renders lamellar crystals of the three polyesters, which display similar features. Thus, truncated lozenge or irregular hexagonal crystals (Figures 6−8) can be observed with dimensions of around 2−15 μm. Correlation of bright-field micrographs and selected area electron diffraction patterns indicates that {120} and {010} are the growth faces, the crystals being elongated along the [100] direction. The growth faces correspond to the planes where molecular chains are

Table 2. Measured and Calculated Electron Diffraction Spacings (nm) for Polyesters 4 *n*

	polyester 4 8		polyester 4 10		polyester 4 12	
index[a]	measd[b]	calcd	measd[b]	calcd	measd[b]	calcd
120	0.415 vs	0.416	0.415 vs	0.415	0.416 vs	0.415
040	0.365 vs	0.365	0.365 vs	0.365	0.366 vs	0.364
140	0.296 w	0.296	0.296 m	0.296	0.294 w	0.295
200	0.253 s	0.253	0.251 s	0.252	0.253 s	0.253
220	0.239 vw	0.239	0.239 m	0.239	0.238 vw	0.239
160	0.219 s	0.220	0.218 s	0.219	0.219 s	0.219
240	0.208 w	0.208	0.206 s	0.207	0.206 w	0.208
080	0.183 m	0.183	0.181 s	0.182	0.181 vw	0.182
260	0.175 vw	0.175	0.175 vw	0.175	0.175 vw	0.175
180	0.172 vw	0.172	0.173 vw	0.172	0.171 vw	0.171
320			0.164 w	0.164	0.164 vw	0.164
340			0.154 vw	0.153		
280			0.148 w	0.148		
1100			0.140 w	0.140		
360			0.139 w	0.139		

[a] On the basis of rectangular unit cells with $a = 0.506$ nm and $b = 1.462$ nm, $a = 0.504$ nm and $b = 1.460$ nm, and $a = 0.506$ nm and $b = 1.456$ nm for polyesters 4 8, 4 10, and 4 12, respectively. [b] Abbreviations denote relative intensities and orientations: vs, very strong; s, strong; m, medium; w, weak; vw, very weak.

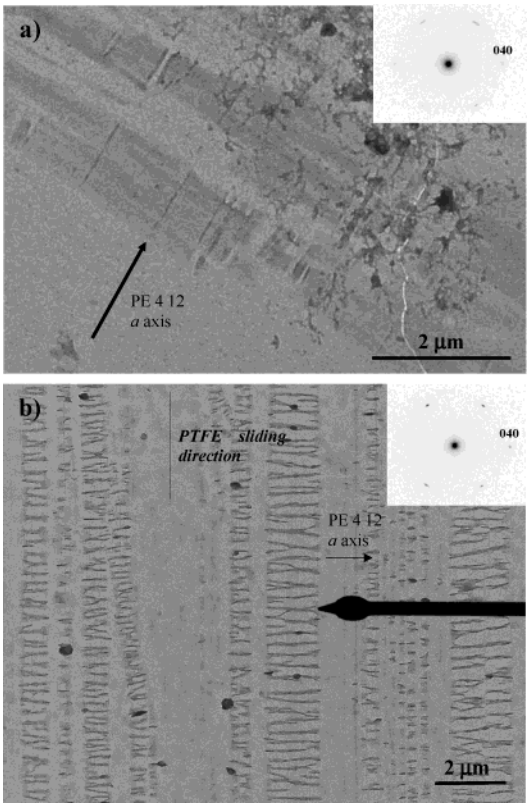

Figure 5. Electron micrographs of the epitaxial growth of polyester 4 12 induced by different substrates. Electron diffraction patterns of the indicated selected areas are shown in the insets. (a) Note the orientation of the polyester growth after dissolution of the benzoic acid substrate. The *b* crystal axis of polyester 4 12 is oriented parallel to the preferential growth direction of the substrate, which corresponds to the direction of the applied temperature gradient for its oriented crystallization. (b) Note that the polyester crystal growth appears oriented perpendicular to the sliding direction of the poly(tetrafluoroethylene) (PTFE) substrate. The *a* crystal axis of polyester 4 12 is perpendicular oriented to the PTFE fiber axis, suggesting the matching between the two crystal lattices since the periodicity between molecular chains of PTFE is close to 0.5 nm.

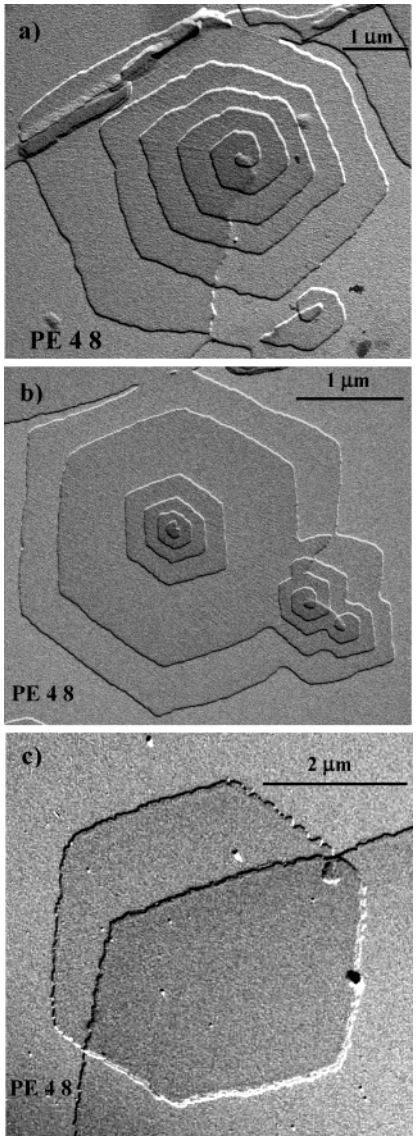

Figure 6. Electron micrographs of lamellar crystals of polyester 4 8 obtained from dilute *n*-hexanol solutions at 50 °C (a) and 45 °C (b, c). Morphologies correspond to truncated lozenge crystals. Spiral growths (a), multilayered crystals (b), and single crystals (c) can be observed in the preparations. Note the presence of two screw dislocations of opposite hand in addition to the terrace growth in micrograph b.

closer. Thus, Figure 2c shows that the linear density is lower along [010] direction compared with the [100] and the [120] directions. The single crystals have two angles close to 110−112° between the {120} growth faces and

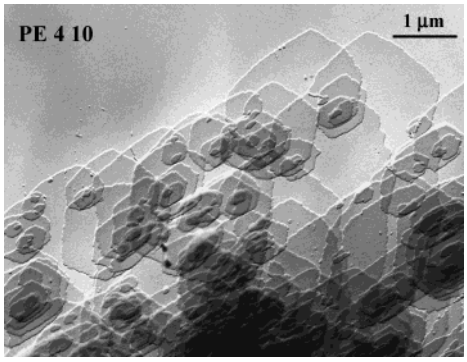

Figure 7. Electron micrograph of polyester 4 10 lamellar crystals obtained from dilute *n*-hexanol solutions at 40 °C. Multilayers are commonly observed, the lamellae having a truncated lozenge morphology and a preferential growth along the [100] direction.

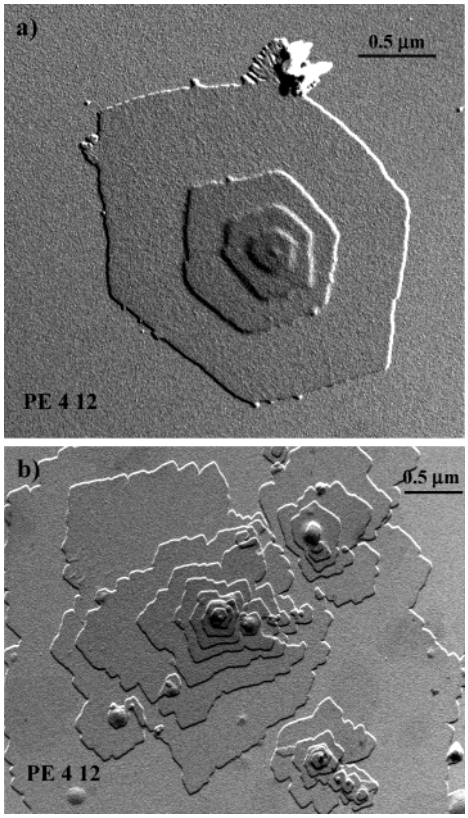

Figure 8. Electron micrographs of polyester 4 12 lamellar crystals obtained from dilute *n*-hexanol solutions. Multilayered crystals with a well-defined habit can be observed at 50 °C (a), whereas highly irregular lamellae are obtained at 30 °C (b).

four angles close to 122−126° between the {120} and {010} growth faces, which match the values of 111 and 125°, respectively, calculated from the unit cell dimensions.

It is possible to obtain large lamellar crystals that contain many layers emanating from screw dislocations (Figure 6a), multilamellar crystals that are grown on a wide base lamella (Figure 6b), and well-developed single crystals (Figure 6c). Aggregates where different lamellae keep a similar orientation can also be found, as shown in Figure 7 for polyester 4 10, where all crystals appear aligned along the crystallographic *a*-axis. Crystallization at high degrees of supercooling (40 °C) leads to irregular crystals, as shown in Figure 8b for polyester 4 12. Microsectorization is produced, and therefore, the {120}

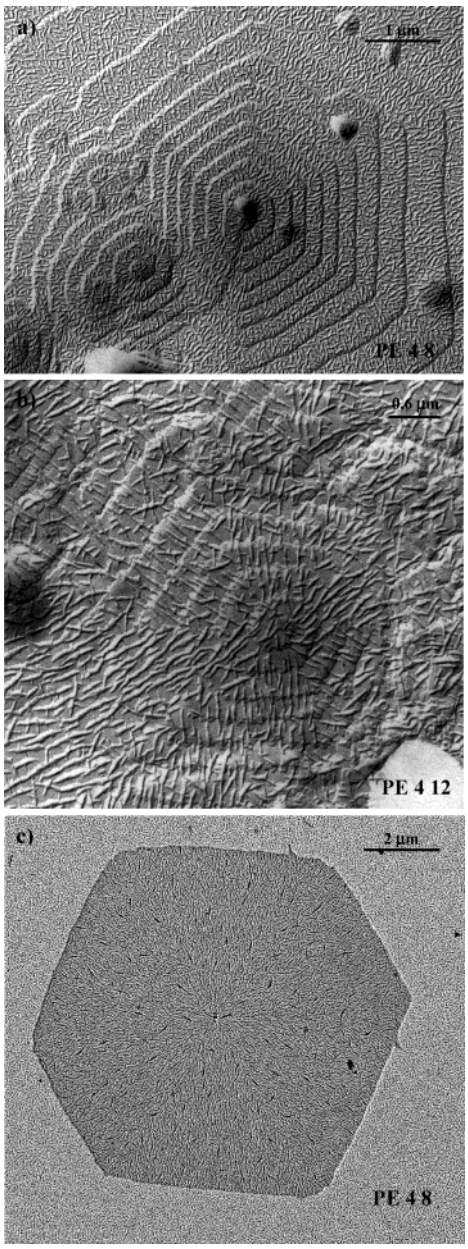

Figure 9. Polyethylene decoration of lamellar crystals of polyesters 4 8 (a) and 4 12 (b). Note that the decoration rods appear with a predominant perpendicular orientation with regard to the crystal growth faces. Samples are shadowed with Pt/C at an angle of 15°. (c) Polyethylene decoration of polyester 4 8 lamellar crystals. In this case, the grid is rotated during shadowing.

growth faces become unstable against the formation of reentrant faces. This feature is well-known in polymer crystallization[38] and indicates that crystallization becomes controlled by diffusion of molecules to the growth front.

All experimental evidence indicates that the studied crystals are essentially flat, the molecular chains remaining oriented perpendicular to the crystal basal plane. Lamellar thicknesses vary in the 6−10 nm range depending on the solvent and especially on the crystallization temperature. These values are determined from both the shadows of crystals measured in the electron micrographs and the lamellar orders observed in the X-ray diffraction patterns of sedimented crystal mats (Figure 3). In the case of polyester 4 12 lamellae obtained from *n*-hexanol at 55 °C, the thickness reached

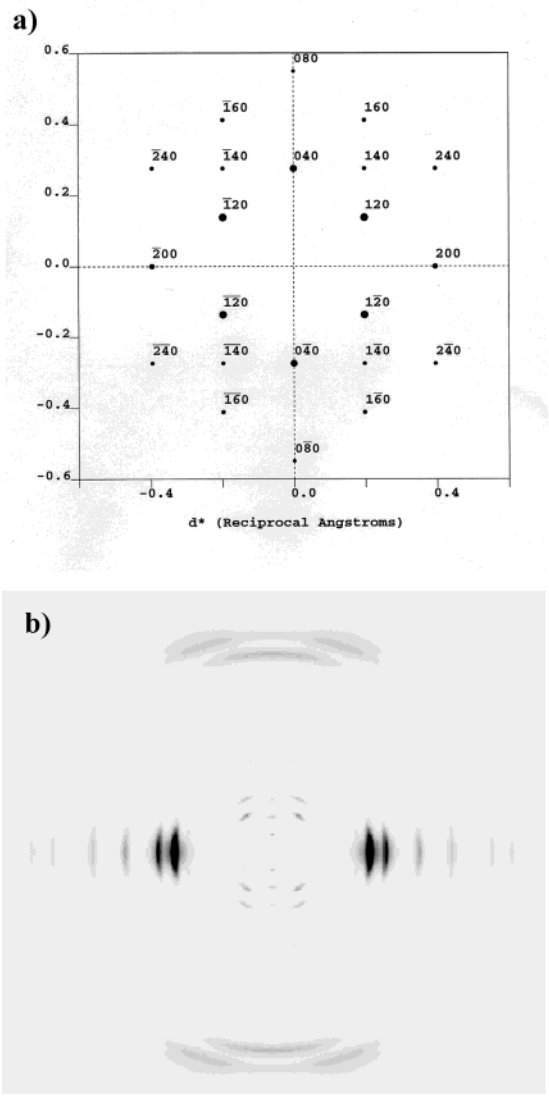

Figure 10. Simulated *hk*0 electron diffraction pattern (a) and X-ray fiber diffraction pattern (b) of the refined structure of polyester 4 12.

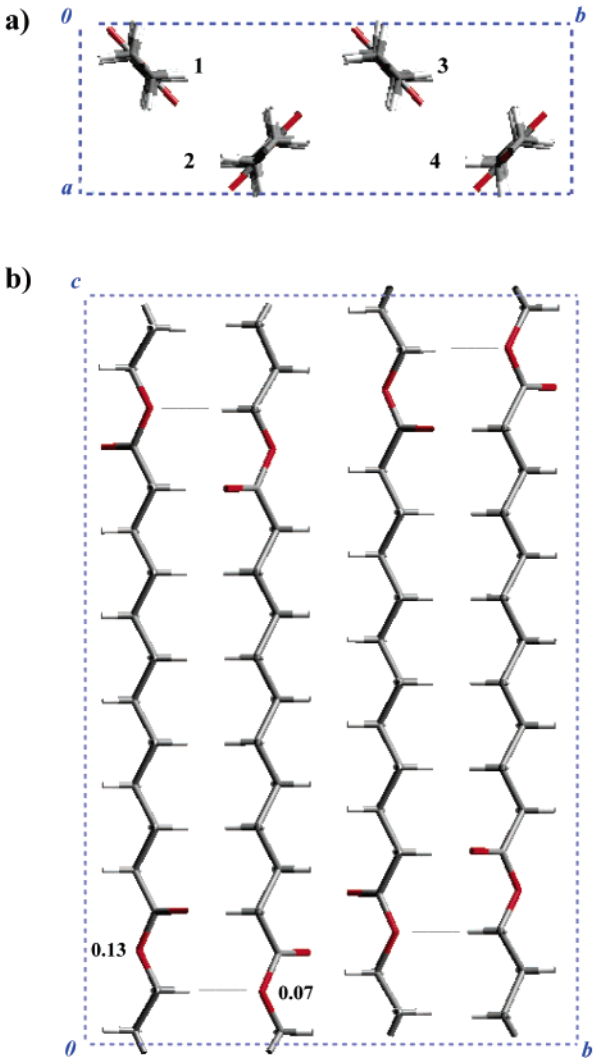

Figure 11. Views of the proposed structure of polyester 4 12: (a) view parallel to the *b*-axis direction; (b) view parallel to the *c*-axis direction. Color code: hydrogen, white; carbon, gray; oxygen, red. The *c*-axial position of molecules 1 and 2 are indicated by the *z* fractional coordinates of the oxygen atoms of diol units. Dashed lines show the alignment between the CH_2 groups and the O atoms of neighboring chains.

a value close to 10 nm, as deduced from the second, third, and sixth lamellar stacking orders that appear with a meridional orientation (Figure 3b). This was also supported by the shadow length in the electron micrograph (Figure 8a). The diffraction pattern is more complex near the fourth and fifth orders due to the presence of the strong 001 reflection. On the other hand, only the first lamellar stacking order can be observed in thin crystals obtained at low crystallization temperatures (Figure 3a).

Polyethylene decoration highlighted the sectorization of the single crystals and also supported a regular folding mechanism.[32] The decorating rods were preferentially deposited perpendicular to the {120} and {010} growth faces (Figure 9), suggesting that the chain folding is parallel to the indicated planes. The shadows of polyethylene rods have different sizes according to their orientation with respect to the Pt/C shadowing source. This feature may cause some sectors to appear more defined than others (Figure 9a,b). To avoid this artificial distinction, the decorated crystals were shadowed as the grid was rotated in the evaporator. Figure 9c clearly shows that all crystal sectors are similarly oriented, although the contrast of the image is reduced.

Structural Modeling. Polyester 4 12 was taken as representative of this series of polymers for the structural modeling because of the better orientation attained in the fiber X-ray diffraction pattern. Molecules were built according to an all-trans conformation and the standard geometry for the bond lengths and angles of polyesters.

In a first step, the azimuthal setting angle (τ) was refined by taking into account the intensities of the experimental *hk*0 electron diffraction patterns. The angle was varied with increments of ±2° from an initial value of 45°. A *P*11*b* space group was assumed, as well as the relationship between the setting angles of molecules 1 and 2 (Figure 2) that gives a *pgg* planar group for the *c*-chain axis projected unit cell ($b = 0.728$ nm).

A minimum *R* factor (15%) was attained with a setting angle of 47°. Values lower than 39° give rise to very weak 200 reflections, whereas the intensity of 040 and 080 reflections appears too weak for angles greater than 55°. Figure 10a shows the simulated *hk*0 electron diffraction pattern, which reasonably agrees with the

Table 3. Observed (F_o) and Calculated (F_c) X-ray Structure Factors for the Refined Model of Polyester 4 12

hkl	d_{measd} (nm)	F_o	F_c[a]
120, $\bar{1}$10	0.415	0.982	0.695, 0.695
040	0.364	0.719	0.588
140, $\bar{1}$40	0.296	0.394	0.261, 0.261
200	0.255	0.495	0.424
220, $\bar{2}$20	0.239	0.162	0.172, 0.172
160, $\bar{1}$60	0.220	0.438	0.378, 0.378
240, $\bar{2}$40	0.209	0.452	0.417, 0.417
001	2.220	0.038	0.039
002	1.110	0.049	0.050
012	0.882	0.085	0.043
003	0.738	0.012	0.056
013	0.659	0.071	0.034
014	0.517	0.035	0.015
015	0.422	0.085	0.040
104	0.377	0.081	0.062
029	0.233	0.252	0.233
039	0.219	0.398	0.264

[a] Calculated by means of the Cerius[2] program. $R = 0.19$.

experimental one. The unit cell projected along the *c*-chain axis is shown in Figure 11a together with the labeling of the different chain segments.

Molecules 1 and 2 were shifted independently along the *c*-chain axis direction, first with steps of 0.05 nm and then with steps of 0.01 nm to fit qualitatively the experimental fiber X-ray diffraction pattern with the simulated one by the Cerius[2] program. Setting angles of −47 and 180−47° were considered for molecule 2, the latter being the most favored angle taking into account the diffraction data. Figure 10b shows the best simulated pattern, which reproduces the main experimental features quite well. In a second step the axial shifts of molecules 1 and 2 were also systematically varied from the above optimized position and the corresponding *R* factors calculated by taking into account the observed and theoretical structure factors. An optimum value of 19% (Table 3) was obtained by applying an additional *c*-axis shift of 0.02 nm to molecule 2. *R* factor increases to 25% when molecules 1 or 2 were independently shifted by ±0.05 nm from the qualitatively refined structure.

A lateral view of the final structure is shown in Figure 11b. It can be seen that the ester groups of molecules 1 and 3 are practically at the same level. The main difference with regard to the smallest unit cell lies in the 180° change between their setting angles. On the contrary, molecule 2 is shifted with respect to molecule 1 in such a way that its CH_2−O methylene groups face the CH_2−*O* oxygen atoms of molecule 1. This kind of interaction between the most electrostatically negative atom (−0.56 for the oxygen atom) and the most electrostatically positive group (0.35 for the indicated CH_2 group) is also found between molecules 3 and 4.

Figure 11b helps also to deduce that the chain folding along both the [120] and [100] directions may take place through the polymethylene segments owing to the small shift between neighboring molecules. Particularly, the decamethylene unit appears more feasible to be involved in the fold than the tetramethylene segment of the diol unit due to its greater length. However, the geometry of the fold must be quite distinct along the two indicated directions, since the setting angles of neighboring molecules are very different. Thus, the molecules are parallel along the [100] direction whereas the setting angles differ in 86° along the [120] direction.

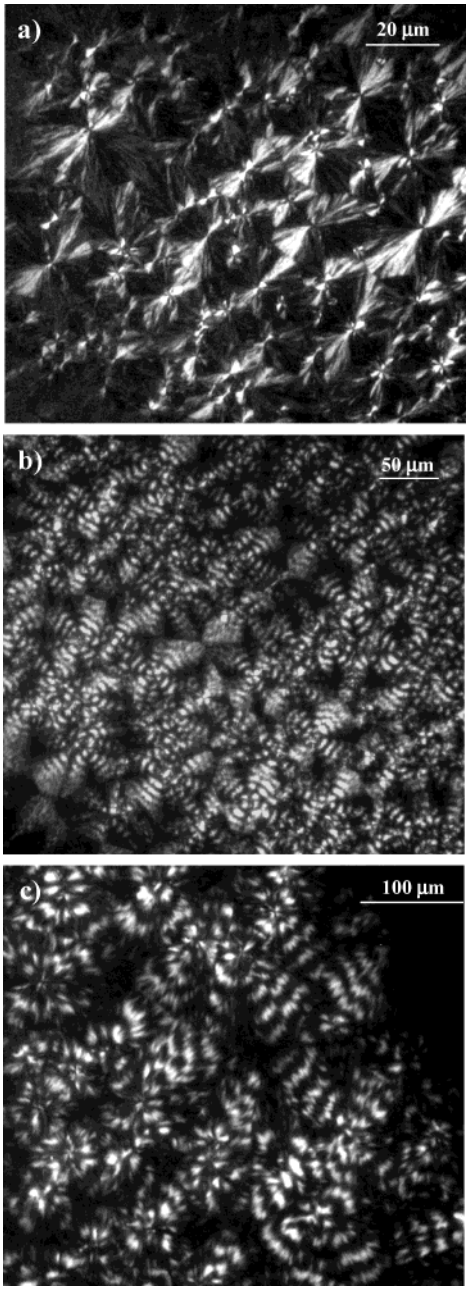

Figure 12. Optical micrographs of polyester 4 10 spherulites crystallized from the melt at 30 °C (a), 40 °C (b), and 50 °C (c).

Melt-Grown Spherulites. Examination of the spherulitic films using a red first-order tint plate showed that the three polymers displayed a negative birefringence; i.e., the direction of the highest refractive index is tangential and hence the molecular axis. We did not observe positively birefringent spherulites in any instances.

The size of polyester spherulites increases with crystallization temperature when the nucleation rate is low compared with the growth rate. Thus, diameters can vary from 20 to 120 μm when crystallization is performed at room temperature or with a low supercooling (10−20 °C), respectively. Figure 12 shows polarized optical micrographs of polyester 4 10 obtained at different temperatures. In addition to the indicated changes in the spherulitic size, it can be observed that ringed spherulites appear when the degree of supercooling decreases. The ring spacing (pitch of the twist) increases

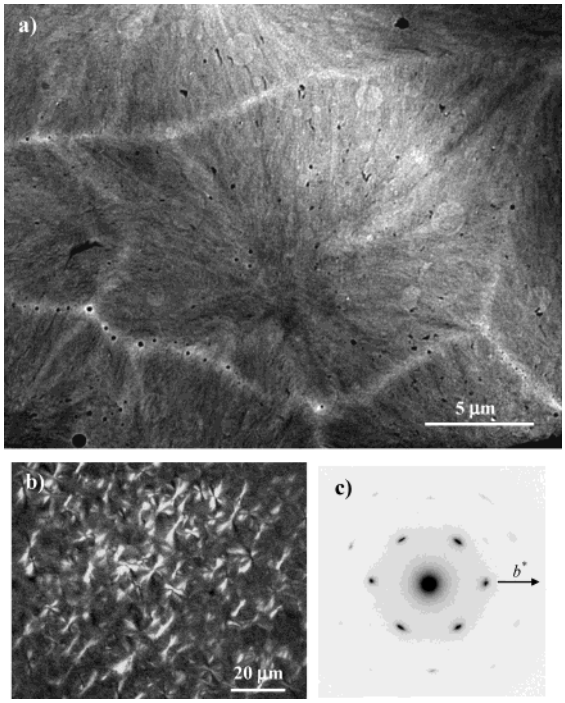

Figure 13. (a) Electron micrograph of polyester 4 12 spherulites obtained by isothermal crystallization at 30 °C from the melt. (b) Optical micrograph of negative birefringent spherulites of polyester 4 12 crystallized from the melt at 30 °C. (c) Electron diffraction pattern of a polyester 4 12 spherulitic film. *a** appears aligned along the spherulitic radius.

with crystallization temperature. This kind of spherulites is a consequence of a lamellar twist that has recently been related to fields generated during the crystal growth process.[39] Spherulites crystallized at low temperatures show a fibrillar texture with two arm extinction pattern when the films are very thin (Figure 12a). Similar observations have been recently reported for ultrathin films of poly(ethylene succinate).[40]

Figure 13shows transmission electron and polarized optical micrographs of polyester 4 12 obtained at 30 °C. The spherulites are characterized by a good fibril-like structure (Figure 13a) grown radially and a Maltese cross or a two black arms extinction pattern (Figure 13b), depending on the thickness of the sample. Our preparation technique allowed to obtain very thin spherulitic films (those that remained adhered to the carbon film), which were consequently suitable for selected area electron diffraction studies. In general, we can get *hk*0 diffraction patterns (Figure 13c) with a 2*mm* symmetry which are similar to those reported for single crystals. Correlation between bright-field micrographs and diffraction patterns indicates that the radial growth direction coincides with the *a* crystallographic axis. The invariance of this kind of pattern confirms the fibrillar structure observed in the electron micrographs.

Conclusions

The results obtained in this work can be summarized as follows:

(1) Polyesters 4 8, 4 10, and 4 12 crystallize as truncated lozenge crystals from dilute *n*-hexanol solutions, their thickness and regularity depending on crystallization temperature.

(2) Polyethylene decoration techniques reveal both that molecules fold along the [100] and [120] crystal directions and that crystals sectorize.

(3) X-ray diffraction data point out that molecular chains have an all-trans conformation and pack according to great unit cells with a double value for the *b* parameter with regard to reported data for similar polyesters. Nevertheless, the *c*-chain axis projection is equivalent to that of conventional unit cells, as deduced from electron diffraction data.

(4) Simulation of both fiber X-ray and electron diffraction patterns demonstrates that packing is defined by a setting angle close to 47°, which is similar to that found in polyethylene. Results may be interpreted according to a *P*11*b* space group symmetry that induces a 180° change between the setting angle of neighboring chains along the *b*-axis direction.

(5) Negative spherulites can be obtained from the melt, their dimensions increasing with crystallization temperature. In addition, the spherulitic texture also changes from fibrillar to ringed with temperature. Observation of ultrathin fibrillar spherulites shows that the *a*-crystal axis is oriented parallel to the spherulitic radius.

Acknowledgment. This research has been supported by the CICYT and FEDER (Grant MAT2003-01004).

References and Notes

(1) Brandrup, J.; Immergut, E. H. *Polymer Handbook*, 3rd ed.; Wiley-Interscience: New York, 1989.
(2) Mark, H.; Stafford, G. *Collected Papers of Wallace Hume Carothers on High Polymeric Substances*; Interscience Publishers: New York, 1940.
(3) Xenopoulos, A.; Clark, E. S. *Nylons Plastics Handbook*; Kohan, M. I., Ed.; Hanser Publishers: Munich, Germany, 1995; Chapter 5.
(4) Huang, S. J. *Encyclopedia of Polymer Science and Engineering*; Wiley-Interscience: New York, 1985; Vol. 2, p 20.
(5) Goodman, I.; Seahan, R. J. *Eur. Polym. J.* **1991**, *26*, 1081.
(6) Stapert, H. R.; Bouwens, A. M.; Dijkstra, P. J.; Feijen, J. *Macromol. Chem. Phys.* **1999**, *200*, 1921.
(7) Paredes, N.; Rodríguez-Galán, A.; Puiggalí, J. *J. Polym. Sci., Polym. Chem. Ed.* **1998**, *36*, 1271.
(8) Paredes, N.; Casas, M. T.; Puiggalí, J.; Lotz, B. *J. Polym. Sci., Polym. Phys. Ed.* **1999**, *37*, 2521.
(9) Model, F. S.; Rochow, E. G. *J. Polym. Sci., Polym. Chem. Ed.* **1970**, *8*, 999.
(10) Chatani, Y.; Suehiro, K.; Okita, Y.; Tadokoro, H.; Chujo, K. *Makromol. Chem.* **1968**, *113*, 215.
(11) De Santis, P.; Kovacs, A. J. *Biopolymers* **1968**, *6*, 299.
(12) Eling, B.; Gogolewski, S.; Pennings, A. J. *Polymer* **1982**, *23*, 1587.
(13) Cartier, L.; Lotz, B.; Ikada, Y.; Tsuji, H.; Puiggalí, J.; Lotz, B. *Polymer* **2000**, *41*, 8909.
(14) Pearce, R.; Brown, G. R.; Marchessault, R. H. *Polymer* **1994**, *27*, 3869.
(15) Puiggalí, J.; Ikada, Y.; Tsuji, H.; Cartier, L.; Okihara, T.; Lotz, B. *Polymer* **2000**, *41*, 8921.
(16) Hu, H.; Dorset, D. L. *Macromolecules* **1990**, *23*, 4604.
(17) Ueda, A. S.; Chatani, Y.; Tadokoro, H. *Polym. J.* **1991**, *2*, 387.
(18) Aylwin, P. A.; Boyd, R. H. *Polymer* **1984**, *25*, 323.
(19) Liau, W. B.; Boyd, R. H. *Macromolecules* **1990**, *23*, 1531.
(20) Kanamoto, T.; Tanaka, K. *J. Polym. Sci., Polym. Phys. Ed.* **1971**, *9*, 2043.
(21) Armelin, E.; Casas, M. T.; Puiggalí, J. *Polymer* **2001**, *42*, 5695.
(22) Armelin, E.; Almontassir, A.; Franco, L.; Puiggalí, J. *Macromolecules* **2002**, *35*, 3630.
(23) Chatani, Y.; Hasegawa, R.; Tadokoro, H. *Polym. Prepr. Jpn.* **1971**, 420.
(24) Ichikawa, Y.; Suzuki, J.; Washiyama, J.; Moteki, Y.; Noguchi, K.; Okuyama, K. *Polymer* **1994**, *35*, 3338.
(25) Ichikawa, Y.; Kondo, H.; Igarashi, Y.; Noguchi, K.; Okuyama, K.; Washiyama, J. *Polymer* **2000**, *41*, 4719.
(26) Minke, R.; Blackwell, J. *J. Macromol. Sci., Phys.* **1979**, *B16*, 407.
(27) Minke, R.; Blackwell, J. *J. Macromol. Sci., Phys.* **1980**, *B18*, 233.

(28) Pouget, E.; Almontassir, A.; Casas, M. T.; Puiggalí, J. *Macromolecules* **2003**, *36*, 698.
(29) Zilberman, E. N.; Kulikova, A. E.; Teplyakov, M. *J. Polym. Sci.* **1962**, *56*, 417.
(30) Miki, K.; Nakatsuka, R. *Rep. Prog. Polym. Phys. Jpn.* **1963**, *8*, 15.
(31) Korshak, V. V.; Vinogradova, S. V. *J. Gen. Chem. U.S.S.R.* **1956**, *26*, 575.
(32) Wittmann, J. C.; Lotz, B. *J. Polym. Sci., Part B: Polym. Phys.* **1985**, *23*, 205.
(33) Wittman, J. C.; Lotz, B. *J. Polym. Sci., Polym. Phys. Ed.* **1981**, *19*, 1853.
(34) Wittman, J. C.; Smith, P. *Nature* 1991, *352*, 414.
(35) *ELD*[2.1], *Quantitative Electron Diffraction*; Calidris: Manhemsvägen 4, Sollentuna, Sweden.
(36) Squire, J.; Al-Khayat, H.; Arnott, S.; Crawshaw, J.; Denny, R.; Diakun, G.; Dover, D.; Forsyth, T.; He, A.; Knupp, C.; Mant, G.; Rajkumar, G.; Rodman, M.; Shotton, M.; Windle, A. *Fibre Diffr. Rev.* **2003**, *11*, 7.
(37) *Cerius*[2]; Accelrys Inc.: Cambridge, U.K.
(38) Basset, D. C.; Keller, A. *Philos. Mag.* **1962**, *7*, 1553.
(39) Schultz, J. M. *Polymer* **2003**, *44*, 433.
(40) Gan, Z.; Abe, H.; Doi, Y. *Biomacromolecules* **2000**, *1*, 713.

MA049939L